frontiers in Marine Science

ORIGINAL RESEARCH
published: 23 July 2020
doi: 10.3389/fmars.2020.00615

Coral Morphology Portrays the Spatial Distribution and Population Size-Structure Along a 5–100 m Depth Gradient

Netanel Kramer[1†‡], Raz Tamir[1,2†‡], Gal Eyal[1,2,3,4†] and Yossi Loya[1†]*

[1] School of Zoology, Tel-Aviv University, Tel Aviv, Israel, [2] The Interuniversity Institute for Marine Sciences of Eilat, Eilat, Israel, [3] ARC Centre of Excellence for Coral Reef Studies, School of Biological Sciences, University of Queensland, St Lucia, QLD, Australia, [4] The Mina & Everard Goodman Faculty of Life Sciences, Bar Ilan University, Ramat Gan, Israel

OPEN ACCESS

Edited by:
Daniel Wangpraseurt, University of Cambridge, United Kingdom

Reviewed by:
Elena Bollati, National University of Singapore, Singapore
Marc Slattery, University of Mississippi, United States

***Correspondence:**
Netanel Kramer
nati.kramer@gmail.com

†ORCID:
Netanel Kramer
orcid.org/0000-0001-5150-0732
Raz Tamir
orcid.org/0000-0002-6988-2510
Gal Eyal
orcid.org/0000-0002-3028-8653
Yossi Loya
orcid.org/0000-0001-6870-9444

‡*These authors have contributed equally to this work*

Specialty section:
This article was submitted to Coral Reef Research, a section of the journal Frontiers in Marine Science

Received: *21 May 2020*
Accepted: *06 July 2020*
Published: *23 July 2020*

Citation:
Kramer N, Tamir R, Eyal G and Loya Y (2020) Coral Morphology Portrays the Spatial Distribution and Population Size-Structure Along a 5–100 m Depth Gradient. Front. Mar. Sci. 7:615. doi: 10.3389/fmars.2020.00615

Population size structure provides information on demographic characteristics, such as growth and decline, enabling *post-hoc* assessment of spatial differences in susceptibility to disturbance. Nevertheless, very few studies have quantified size data of scleractinian corals along a shallow-mesophotic gradient, partly because of previously inaccessible depths. Here, we report the coral size-frequency distributions at the morphology level (six growth forms) and at the species level for ten representative locally abundant species along a broad depth gradient (5–100 m) in the Gulf of Eilat/Aqaba (GoE/A). A total of 18,865 colonies belonging to 14 families and 45 genera were recorded and measured over four reef sites. Colonies were found to be 11.2% more abundant at mesophotic (40–100 m; 55.6%) depths compared with shallow (5–30 m; 44.4%). The coral taxa exhibited heterogeneity in their size-structure, with marked differences among depths, morphological growth forms, and species. Branching and corymbose corals were more prevalent in shallow waters, while encrusting and laminar forms comprised the majority of mesophotic corals. Nevertheless, massive morphology was the most abundant growth form across all sites and depths (39%), followed by laminar (26%) and encrusting (20%). Corymbose corals (primarily Acroporidae) revealed constrained size at all depths; with the lack of small-size groups indicating populations at risk of decline. Depth-generalist species belonging to massive and laminar morphologies generally exhibited a larger colony size at the mesophotic depths, but were typified by a higher number of small colonies. Furthermore, we refute the widely and long-accepted assertion that *Stylophora pistillata* is the most abundant coral in the northern GoE/A, and assert that *Leptoseris glabra* is the one. Here, we provide a baseline for future monitoring of coral population structures, insights to recent ecological dynamics, retrospective assessment of coral community recovery following disturbances and grounds for conservation assessments and management actions.

Keywords: coral reefs, mesophotic coral ecosystems (MCEs), size-frequency distributions, population structure, growth forms, morphology, Gulf of Eilat/Aqaba

INTRODUCTION

Coral reefs encompass diverse and complex organisms that inhabit broad environmental gradients world-wide. For scleractinian corals, spatial differences in abiotic regimes (e.g., light, temperature, hydrodynamic, etc.) and/or impact by disturbances may influence their distribution and population dynamics (Bauman et al., 2013; Dubé et al., 2017; Osborne et al., 2017; Lesser et al., 2018). For example, it was recently demonstrated that variation in coral community structure is correlated with changes in light conditions across shallow-to-mesophotic environments (Tamir et al., 2019).

Community demographic mechanisms in scleractinian corals are commonly assessed according to size-frequency distributions (SFDs), and can vary widely within and among coral populations (Bak and Meesters, 1998; Dubé et al., 2017). Studying various size-classes in corals may yield valuable insights into processes of their life history (Bak and Meesters, 1998; Anderson and Pratchett, 2014), and the analyses of these size-classes may serve as a better indicator of reef health and stability than other common metrics, such as coral cover or diversity (Bak and Meesters, 1999; Smith et al., 2005). Ecological processes occurring at the population level are strongly related to size and can provide information about recruitment, fecundity, mortality, and population responses to stressful environmental conditions (Hughes and Jackson, 1985; Baird and Marshall, 2002; Neal et al., 2017; Kramer et al., 2019). Furthermore, these processes are directly linked to the species' inherent life-history traits, such as reproductive strategy and maturity, colonization characteristics, growth, and longevity (Darling et al., 2012; Anderson and Pratchett, 2014; Adjeroud et al., 2015). Thus, any change in one of these traits could alter the population structure and impair its resilience to local and/or global climate-driven changes, which could eventually reshape the reef habitat (Darling et al., 2013; Hughes et al., 2018b; Shlesinger and Loya, 2019).

The SFD pattern of several coral populations has been shown to be negatively skewed, with populations or species-specific corals comprising mainly larger colonies and relatively few smaller ones, which in turn hinders the recovery of these populations following disturbances, while less impacted populations display a positive skew (Bak and Meesters, 1998, 1999). This may be indicative of a population at risk of decline due to unsuccessful recruitment or impaired reproductive performances (Shlesinger et al., 2018; Shlesinger and Loya, 2019). However, the degree of skewness may vary among coral species and can shed light on their life-history strategy (Adjeroud et al., 2015). Likewise, the skewness may be biased by a variation in colony size within and among species at different depths (Adjeroud et al., 2007; Einbinder et al., 2009). Scleractinian corals exhibit high levels of variation in coral growth morphology within and among taxa (Pratchett et al., 2015; Zawada et al., 2019). Coral growth forms directly dictate life-history strategies, and are influenced by depth, due to the strong effect of light in enhancing coral calcification (Goreau, 1959). Furthermore, the mortality and susceptibility of corals to different environmental disturbances are strongly linked to their morphological growth form (Loya et al., 2001; Torda et al., 2018), which in turn impacts their spatial and size distributions.

Following the accelerating deterioration in coral reefs worldwide over recent decades (Hughes et al., 2018a), efforts to prevent corals from extinction are increasing. Effective reef management must, therefore, be based on in-depth knowledge regarding the reef's state of health and the environmental variables that may affect it. As part of the search for reliable and appropriate resources to promote the resilience and recovery of shallow-water degraded reefs, increased interest has been focused in the last decade on mesophotic coral ecosystems (MCEs) (Loya et al., 2016, 2019; Turner et al., 2017). MCEs are light-dependent communities usually found between 30–40 m and 150 m depth (Hinderstein et al., 2010). These deep reefs were previously considered to be more resilient than shallow reefs to perturbations and were suggested to have the potential to serve as natural refuges for certain shallow-reef species and potentially re-seed disturbed shallow reefs (Glynn, 1996; Bongaerts et al., 2010). However, a growing body of literature currently indicates that the mesophotic environments themselves are not immune to disturbances (Rocha et al., 2018). Mesophotic corals impacted by tropical storms can be smothered beneath sediment and suffer physical damage, as well as impacted by extreme heatwaves that lead to coral bleaching. Since depth is a well-known factor affecting coral growth, it is expected that the recovery rate from disturbances may differ along a depth gradient (Rocha et al., 2018; Pinheiro et al., 2019). With increasing depth, coral individuals exhibit a decline in their linear extension and calcification rate, due to decreasing levels of photosynthetically-active radiation (Pratchett et al., 2015). Subsequently, stronger negative impacts on MCEs could affect the restoration of their population structures due to slower growth rates (Pinheiro et al., 2019).

While it has been demonstrated that mesophotic scleractinian corals (∼30–150 m) thrive under limited light and constitute a major component of coral reefs (Eyal et al., 2019; Pyle and Copus, 2019), the ecological and biological processes driving their distribution and population structure have remained insufficiently studied worldwide, including in the otherwise highly investigated mesophotic reefs of the Gulf of Eilat/Aqaba (GoE/A) (Turner et al., 2017). Although SFD is one of the most appropriate methods for studying coral demographics, its use to date has been limited to the shallow reefs and performed mostly at a single depth (Bauman et al., 2013; Anderson and Pratchett, 2014; Adjeroud et al., 2015; Shlesinger and Loya, 2019), or focused on only one genus or growth form along a wide depth gradient (Vermeij and Bak, 2003; Goodbody-Gringley et al., 2015).

Here, we present a comprehensive investigation of the spatial and size-frequency distributions of locally abundant ten coral species representing six common morphological categories along a wide depth gradient (5–100 m), in the GoE/A. Such information may provide an indication regarding the dynamics and impact of both natural and anthropogenic factors on the health and stability of the coral community as a whole. To this end, the aims of this study were to: (1) quantitatively characterize coral SFDs and depth occupation of various growth forms and species; and

(2) determine whether coral size is randomly distributed at and among various growth forms, species, and depths.

MATERIALS AND METHODS

Study Sites

The coral reef of Eilat cover proximately 11 km of fringing and patchy type reefs, extending from the water surface down to 140 meters depth (Fricke and Schuhmacher, 1983), and, although being among the most northern reefs worldwide, are characterized by spectacular and diverse stony corals (Loya, 2004). These reefs are located at the northern tip of the Red Sea, near the city of Eilat, Israel (29° 55'N/34° 95'E), a city with a population of 52,000. The city's coastline features industrial complexes, commercial and military ports, agricultural runoff, recreational marinas, as well as a thriving tourist industry. Moreover, natural stressors (e.g., flash-flood events – Katz et al., 2015; southern storms – Eyal et al., 2011) are exposing the reef to various anthropogenic disturbances which are expressed in various magnitudes at different sites along the city's shore, such as eutrophication, agricultural waste, light pollution, and diving activities (Zakai and Chadwick-furman, 2002; Loya, 2004, 2007; Tamir et al., 2017). Additionally, due to the extremely steep slope, the reef skirts the shoreline at an unusually close range of only a few meters from the disturbances deriving from the city (Loya, 2004).

The Gulf of Eilat/Aqaba is located in a (semi-arid) desert area, characterized by very minimal river runoff, leading to low water turbidity (Katz et al., 2015), and low nutrient concentration and phytoplankton biomass (Lazar et al., 2008). These natural conditions allow sunlight to reach and penetrate the water body to considerable depths (i.e., a yearly average of 1% photosynthetically active radiation (PAR) from the surface at ∼80 m depth) (Tamir et al., 2019). Nonetheless, as a result of the natural and anthropogenic disturbances, the water properties along the shore are not uniform (Tamir et al., 2019). Hence, there is variability in light attenuation (K_dPAR) along the city shore (e.g., 0.07 K_dPAR at our northern site, near the city of Eilat, compared to 0.05 K_dPAR, 10 km southward at our most southern site), expressed in critical differences in light regime among sites (see Tamir et al., 2019).

Ecological Community Surveys

Spatial benthic surveys were conducted during 2017–2018 over 10 km of the reef at four sites from the shallow reef down to the MCE (0–100 m depth). Belt transects, 50 m in length, were recorded at seven depths (5, 10, 20, 30, 40, 50, and 60 m) using photography in technical-diving, and at 70–80 and 90–100 m, using a drop-camera system – a photo-quadrant-pod frame tethered to the boat with a coaxial cable providing a live view video, and a custom-made lighting system. A dive computer was connected to the frame to confirm depth parallel to the shoreline along the isobaths at each site. To avoid parallax error, leading to under- or over-estimation in size, both diving and drop camera transects were conducted using a similar size and height photo-quadrant-pod frame with a static fixed camera on the top parallel to the reef bottom (see Pratchett et al., 2015). Each photo was taken while the quadrat-pod was placed perpendicular to the reef surface.

Out of 70 photo-plots at each site and depth, 30 photo-plots (70 × 50 cm) were randomly selected to record the size and abundance of coral taxa, for community structure and SFD analysis. Colony size was determined for the living surface according to the projected surface area (cm^2) of each colony within the area of each quadrat, and measured using Photoshop software (Photoshop CS6, Adobe Inc.). Although three-dimensional surface area and volume are important metrics of size and growth, our decision to measure the projected planar area was based on Pratchett et al. (2015), which states this as an appropriate method for the study of coral demography. Furthermore, this method was suggested to serve as an effective proxy for the three-dimensional colony (House et al., 2018). The smallest colony size detectable (1 cm^2) was determined based on the ability to identify the coral at the genus level. This size category was determined consistently between both diving and drop camera methods. The photo-plots frame was used as a scaling reference (Pratchett et al., 2015). Each colony count was based on the condition that either all or the center of the colony was within the quadrat (Zvuloni et al., 2008). Due to the difficulty of accurately assessing the species identity of some corals from photos, coral taxa were classified at either the genus or species level, based on the authors' experience and knowledge, with assistance from the literature. Each coral taxon was assigned to one of six coral growth forms (branching, corymbose, digitate, encrusting, laminar, or massive) based on the Coral Trait Database website[1] (Madin et al., 2016).

Environmental Parameters

A distance-based linear model (DistLM) routine in the software PRIMER v7 (Clarke, 1993) examined the associations between the response variables (logarithmic size groups) that could be explained by a set of explanatory variables (environmental parameters). Environmental data (temperature, salinity, chlorophyll-*a*, and oxygen) were provided by the national monitoring program (NMP) of the Gulf of Eilat from 2017 (NMP, 2017), and photosynthetically active radiation (PAR) data were taken from Tamir et al. (2019). Data were averaged and normalized prior to the analysis, due to their featuring different units and scales.

Statistical Analyses

Statistical analyses were performed using the R software (R Core Team, 2020). Analyses were performed on two scales: (1) morphological categories, which were performed on all the identified species within the transects; and (2) representative species from each category: Branching (*Stylophora pistillata* and *Acropora squarrosa*); Corymbose (*Acropora valida*); Digitate (*Pavona cactus*); Encrusting (*Leptoseris incrustans* and *Montipora meandrina*); Laminar (*Leptoseris fragilis* and *Montipora danae*); and Massive (*Montipora informis* and *Paramontastrea peresi*). All these species, except *Leptoseris* spp. corals, are depth-generalists

[1] http://coraltraits.org

(i.e., abundant throughout the entire depth range; Tamir et al., 2019). The SFDs were given as a percentage of all colonies within each growth form or species, and data were transformed to a logarithmic scale (by log10; $mean_{log}$) to normalize the distributions and increase resolution within smaller size-classes. Data were then analyzed using descriptive statistical measures of size hierarchies: the coefficient of variation (CV), in which significantly low values suggest constrained body size, and increased CV indicates expansion in size diversity; skewness (g_1), which indicates the relative abundance of small and large colonies within a population; and kurtosis (g_2), which identifies whether the tails of a given distribution contain extreme values. The normality of the SFDs was assessed for the transformed data using Shapiro-Wilk (SW) tests, and the significance of skewness and kurtosis were assessed by dividing g_1 and g_2 by their respective standard errors to obtain the test statistics, following Cramer (1997). The geometric mean size (projected surface area; $mean_g$) and the 95% percentile (the maximum colony size reached within a population; Q95) were also calculated. The $mean_{log}$ distribution was compared among depths and growth forms/species using the non-parametric k-sample Anderson-Darling (AD) test, with the null assumption that all samples came from the same distribution; and two-sample Kolmogorov-Smirnov (KS) tests were used to determine whether any two distributions differed from one another. *P*-values for multiple testing were adjusted based on the Bonferroni correction method in SW and KS tests.

Variations in the above parameters were analyzed using mixed-effects permutational analysis (MEPA; 1000 permutations), and *site* was considered a random factor to account for the lack of some species at certain sites. Species with less than three individuals per depth (pooled among sites) were excluded from the analyses. Finally, changes in the composition of growth form communities at the genus level were visualized using non-parametric multidimensional scaling (NMDS) using a Bray-Curtis dissimilarity matrix, created by the {vegan} R package (Oksanen et al., 2018). The analyses were run using the R packages {lme4} (Bates et al., 2015) and {predictmeans} (Luo et al., 2014), and permutational *t*-tests were run with {RVAideMemoire} package (Hervé, 2019).

RESULTS

Spatial Distribution and Composition

A total of 18,865 colonies belonging to 14 families and 45 genera were detected and measured over the four surveyed reef sites. Colonies were found to be more abundant at mesophotic depths (40–100 m; 55.6%) than shallow depths (5–30 m; 44.4%). Percentages were normalized according to the sampling effort between the depth zones (shallow: 193 quadrats; mesophotic: 213 quadrats). A third of the colonies (33.2%) were recorded in mid-reef habitats (30–40 m), while the lowest abundance was found at 100 m (2.3%). The survey revealed that *Leptoseris glabra* was the most abundant coral species overall at all depths and sites (10.7%), although it was predominantly found at mesophotic depths. *Leptoseris* species also stand out as the most abundant coral at the genus level in the GoE/A (21.8%), followed by *Alveopora* (10.2%), *Montipora* (7.1%), *Porites* and *Stylophora* exhibiting equal contributions of 6% each. Within the shallow sites, the most abundant coral species were: *S. pistillata* (10.6%), *Porites* spp. (7.6%), and *P. peresi* (4.3%), whereas at the mesophotic depths, *L. glabra* (19.8%), *Alveopora* spp. (12.8%), and *L. fragilis* (9.7%; mainly at 70–100 m) were the most common.

Overall, the site with the richest coral abundance was the Nature Reserve, with more than a quarter of all the corals found there. Additionally, a noticeable variability in the depth abundance patterns was detected for most corals, with distinct assemblages according to growth forms (MEPA, $p < 0.01$; **Figure 1A**). While species such as *S. pistillata, M. meandrina, M. danae,* and *P. peresi* exhibited broad spatial distribution patterns, other species, such as *P. cactus,* were characterized largely by local distributions at specific sites and

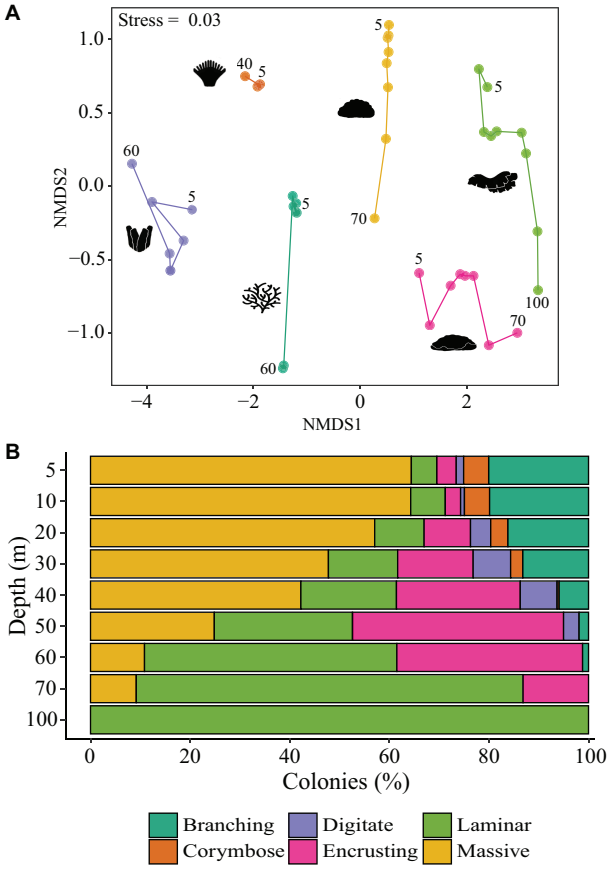

FIGURE 1 | (A) NMDS ordination plot based on Bray-Curtis dissimilarity matrices (2D, stress = 0.03). Each color represents a particular growth form category and each dot the assemblage composition at genus-level for a given depth and morphological category (pooled by sites). Dots are connected by consecutive depths (m), and numbers on the edges of each line denote the shallowest and deepest depths for a given morphological category; **(B)** Total cumulative percentage of the relative abundance of the six growth form categories (branching, corymbose, digitate, encrusting, and laminar, massive) along a depth gradient ranging from 5 to 100 m.

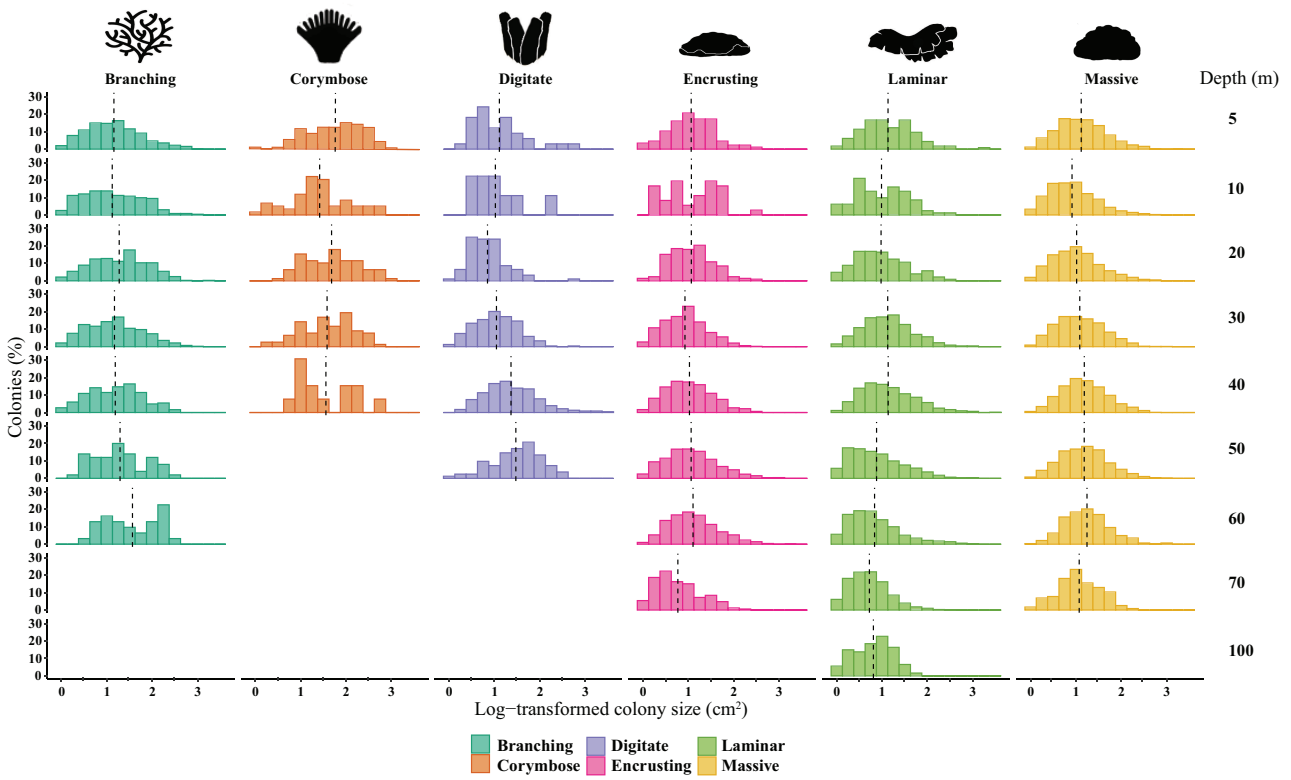

FIGURE 2 | Size-frequency distributions (SFDs) based on log-transformed size classes of six morphological categories: branching, corymbose, digitate, encrusting, laminar and massive across depths (5, 10, 20, 30, 40, 50, 60, 70, and 100 m; pooled among sites). Dashed black lines indicate $mean_{log}$, and colors denote the different morphological categories.

depths. Massive morphology was the most abundant growth form across all sites and depths (39%), followed by laminar (26%) and encrusting (20%) (**Figure 1B**). The occurrence of morphological forms changed significantly with depth (MEPA, $p < 0.001$; **Figure 1**). Branching, corymbose, and digitate corals were limited to 5–60 m depth, whereas the other growth forms were found also at 70 and 100 m. Corymbose and branching colonies were primarily found at shallow depths (< 30 m), becoming significantly reduced with increasing depth, where laminar and encrusting corals became the prevailing morphologies (**Figure 1B**).

SFDs of Morphological Categories

The SFDs varied among and within coral morphologies, as well as along the depth gradient (AD test, $p < 0.001$; **Figure 2**). Due to the high variability and low occurrences of individuals at certain sites, the data were pooled among sites for the statistical analyses. Nearly half (48%) of all colonies fell within the small-size classes (1–20 cm^2), with 54% of them found at shallow sites. Overall, the mean colony surface projected area ($mean_g$) decreased with depth (pooled across growth forms and sites), and varied among the six growth categories (MEPA, $p < 0.001$). Corymbose corals had the largest $mean_g$ size recorded across all depths ($mean_g$ = 78-125 cm^2; **Supplementary Figure S1**), differing by one order of magnitude from all the other growth forms, and displaying the overall largest colony (Q95 = 564 cm^2 at 20 m depth). In contrast, laminar and encrusting assemblages displayed $mean_g$ values lower than 50 cm^2. With the exception of the corymbose and encrusting morphologies, all the other growth types showed a significant size variability with depth (permutational *t*-test, $p < 0.01$, **Table 1**).

SFDs differed between certain depths within a growth form, as indicated by significant pairwise KS tests ($p < 0.05$; **Supplementary Table S1**). Only the SFD of the corymbose assemblages presented normal distributions across all depths (Shapiro-Wilk test > 0.05) and generally exhibited lower dispersions of the size data, as indicated also by the low coefficient of variation (CV = 33.95–47.56). The majority of the morphological assemblages were characterized by potentially a-symmetrical size distributions (g_1: 0.263–1.219; $p < 0.05$; **Figure 3** and **Table 1**). For most of the morphological assemblages (excluding corymbose and some branching corals), the SFDs were positively skewed along the depth gradient according to log-transformed colony-size data, reflecting a preponderance of colonies of smaller-size classes (**Table 1**). All corymbose corals exhibited symmetrical distributions, while branching corals were positively skewed mostly at shallow depths. Most (77%) of the assemblages displayed mesokurtic distributions (normal-like tails), while a few distributions

FIGURE 3 | Size-frequency distributions (SFDs) based on untransformed size classes (cm^2) of six morphological categories: branching, corymbose, digitate, encrusting, laminar and massive across depths (5, 10, 20, 30, 40, 50, 60, 70, and 100 m; pooled among sites). Data were distributed among seven size classes (0–5, 5–10, 10–20, 20–30, 30–40, 40–50, 50+; cm^2).

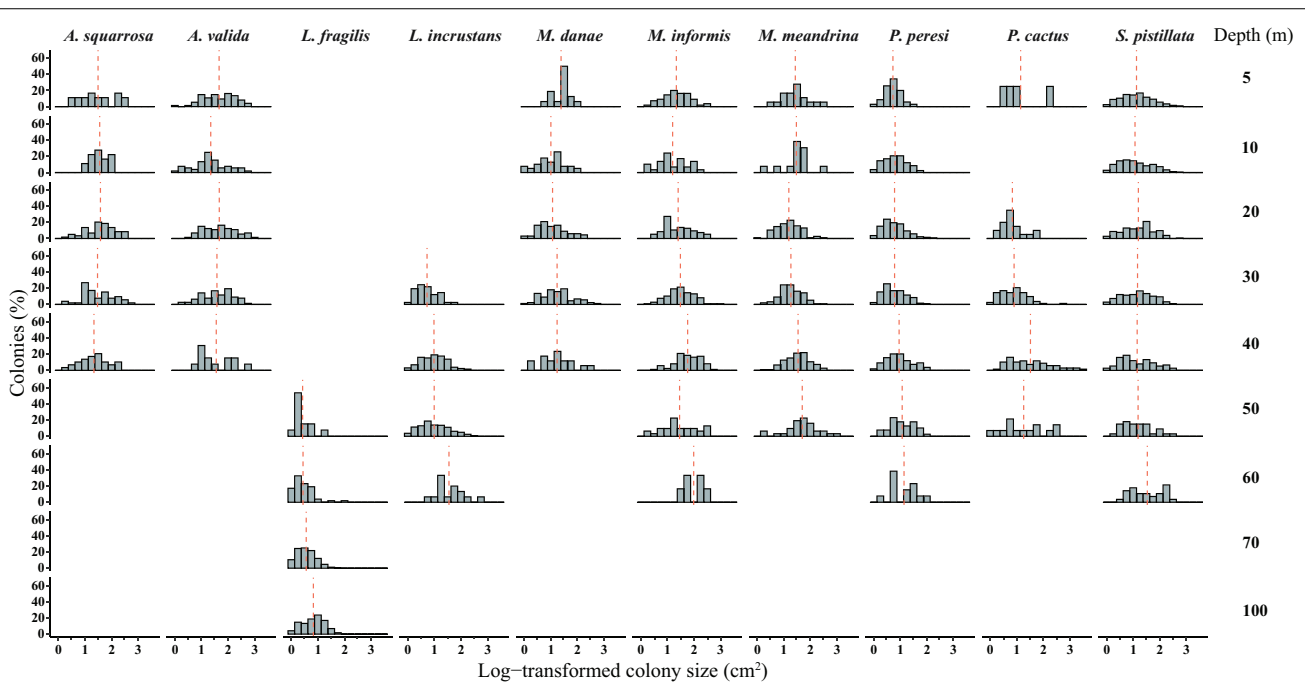

FIGURE 4 | Size-frequency distributions (SFDs) based on log-transformed size classes of ten representative locally abundant species: *A. squarrosa*, *A. valida*, *L. fragilis*, *L. incrustans*, *M. danae, M. informis, M. meandrina, P. peresi, P. cactus,* and *S. pistillata* across depths (5, 10, 20, 30, 40, 50, 60, 70, and 100 m; pooled among sites). Dashed orange lines indicate $mean_{log}$.

displayed either negative or positive kurtosis. Only branching corals exhibited varying kurtosis values across depth, with platykurtic (negative kurtosis) distributions at 10, 20, and 40 m (**Table 1**). Lastly, the DistLM test revealed that only light (PAR) had a significant correlation to the size-distribution of all the environmental parameters, although its contribution to the variation was small (DistLM, *Prop.* = 0.096, $p < 0.01$).

TABLE 1 | Basic statistical summary of untransformed data (white background) and statistical summary of SFD log-transformed colony size (shaded background) based on six growth forms.

Growth form	Depth (m)	*n*	Mean$_g$ (SE)	%	Q95	Mean$_{log}$ (SE)	g_1 (Stat)	g_2 (Stat)	CV	*p*
Branching	5	447	42.52 (4.28)	20.1	202.58	1.16 (0.03)	0.45 (3.91)	−0.23 (−0.98)	52.58	**0.00**
	10	232	39.95 (5.50)	19.9	140.72	1.12 (0.04)	0.32 (2.02)	−0.70 (−2.21)	57.45	**0.00**
	20	367	48.21 (5.6)	16.2	165.99	1.27 (0.03)	0.03 (0.26)	−0.60 (−2.37)	47.99	**0.03**
	30	418	41.91 (4.58)	13.2	189.00	1.17 (0.03)	0.30 (2.55)	−0.46 (−1.91)	52.48	**0.00**
	40	183	37.11 (4.27)	5.9	171.39	1.19 (0.04)	0.12 (0.67)	−0.73 (−2.04)	50.06	0.19
	50	50	46.50 (9.39)	1.9	183.91	1.29 (0.08)	0.28 (0.83)	−0.90 (−1.36)	45.41	0.27
	60	31	83.48 (17.87)	1.2	229.41	1.57 (0.11)	0.06 (0.14)	−1.37 (−1.67)	38.98	0.33
Corymbose	5	112	125.50 (14.63)	5.0	418.23	1.76 (0.06)	−0.28 (−1.23)	−0.65 (−1.44)	33.95	0.36
	10	59	78.49 (17.09)	5.1	387.24	1.42 (0.09)	0.02 (0.07)	−0.28 (−0.45)	47.56	1.00
	20	78	120.54 (20.36)	3.4	564.37	1.68 (0.07)	0.14 (0.50)	−0.83 (−1.54)	36.53	0.94
	30	77	80.01 (11.61)	2.4	296.25	1.58 (0.07)	−0.26 (−0.93)	−0.48 (−0.88)	36.46	1.00
	40	13	88.61 (34.96)	0.4	308.33	1.56 (0.17)	0.55 (0.90)	−1.28 (−1.07)	39.11	0.45
Digitate	5	33	43.42 (17.62)	1.5	253.71	1.11 (0.10)	1.14 (2.80)	1.09 (1.37)	53.01	**0.05**
	10	9	25.31 (14.67)	0.8	96.88	1.02 (0.19)	0.91 (1.27)	0.70 (0.50)	55.47	1.00
	20	92	15.49 (5.9)	4.1	32.94	0.85 (0.04)	1.22 (4.58)	3.73 (7.49)	48.77	**0.00**
	30	238	22.02 (3.41)	7.5	56.88	1.04 (0.03)	0.25 (1.60)	0.01 (0.04)	46.00	0.21
	40	229	84.88 (18.95)	7.4	271.89	1.36 (0.04)	0.74 (4.58)	0.76 (2.38)	43.87	**0.00**
	50	82	56.22 (7.17)	3.1	182.52	1.47 (0.06)	−0.43 (−1.63)	−0.15 (−0.29)	37.15	1.00
Encrusting	5	87	24.94 (5.50)	3.9	80.27	1.06 (0.05)	0.41 (1.57)	0.50 (0.98)	46.83	1.00
	10	36	28.78 (10.10)	3.1	57.18	1.07 (0.10)	0.29 (0.73)	−0.45 (−0.59)	53.65	0.62
	20	211	22.57 (2.49)	9.3	71.73	1.07 (0.03)	0.42 (2.51)	−0.12 (−0.35)	44.43	0.09
	30	480	16.11 (1.18)	15.2	60.61	0.93 (0.02)	0.37 (3.28)	−0.15 (−0.69)	50.85	**0.00**
	40	771	22.95 (1.46)	24.9	81.52	1.03 (0.02)	0.40 (4.50)	−0.25 (−1.40)	50.15	**0.00**
	50	1117	33.15 (2.67)	42.4	131.25	1.06 (0.02)	0.52 (7.10)	0.09 (0.62)	54.14	**0.00**
	60	970	30.68 (2.25)	37.3	122.13	1.10 (0.02)	0.53 (6.73)	−0.01 (−0.06)	48.19	**0.00**
	70	166	12.19 (1.6)	13.1	45.86	0.77 (0.04)	0.61 (3.24)	0.00 (0.00)	63.56	**0.00**
Laminar	5	114	47.09 (18.98)	5.1	101.84	1.13 (0.05)	0.64 (2.81)	1.10 (2.45)	50.58	0.21
	10	81	23.92 (5.33)	6.9	73.39	0.99 (0.06)	0.35 (1.30)	−0.46 (−0.87)	57.57	0.81
	20	225	23.47 (2.68)	9.9	111.17	0.98 (0.04)	0.47 (2.92)	−0.45 (−1.38)	57.66	**0.00**
	30	440	33.10 (3.88)	13.9	124.12	1.12 (0.03)	0.49 (4.24)	0.20 (0.88)	47.73	**0.00**
	40	595	45.88 (6.07)	19.2	173.81	1.13 (0.02)	0.67 (6.71)	0.23 (1.15)	52.89	**0.00**
	50	731	25.39 (2.95)	27.7	103.70	0.88 (0.02)	0.79 (8.75)	0.20 (1.11)	67.59	**0.00**
	60	1318	24.61 (2.15)	50.6	106.35	0.83 (0.02)	1.05 (15.65)	1.03 (7.67)	69.15	**0.00**
	70	981	9.95 (0.66)	77.7	33.26	0.72 (0.01)	0.72 (9.28)	0.64 (4.13)	60.33	**0.00**
	100	428	9.91 (0.47)	100.0	28.63	0.81 (0.02)	−0.06 (−0.55)	−0.81 (−3.34)	51.99	**0.00**
Massive	5	1436	30.69 (2.08)	64.4	116.73	1.12 (0.01)	0.38 (5.86)	−0.07 (−0.54)	47.65	**0.00**
	10	751	19.94 (1.68)	64.3	73.59	0.91 (0.02)	0.66 (7.43)	0.31 (1.76)	56.67	**0.00**
	20	1293	25.69 (1.65)	57.1	96.60	1.01 (0.01)	0.57 (8.40)	0.18 (1.33)	52.39	**0.00**
	30	1512	26.14 (1.46)	47.8	95.27	1.08 (0.01)	0.33 (5.29)	−0.26 (−2.06)	47.29	**0.00**
	40	1310	30.88 (1.36)	42.2	114.62	1.18 (0.01)	0.28 (4.13)	−0.24 (−1.77)	42.22	**0.00**
	50	655	32.93 (2.51)	24.9	120.76	1.18 (0.02)	0.26 (2.76)	−0.14 (−0.73)	43.88	**0.03**
	60	282	40.68 (6.11)	10.8	137.60	1.24 (0.03)	0.53 (3.68)	0.48 (1.65)	40.67	**0.01**
	70	116	20.97 (2.51)	9.2	68.99	1.07 (0.04)	0.06 (0.25)	−0.33 (−0.75)	44.02	1.00

The sample size (n); geometric mean size (Mean$_g$; cm^2), and standard error (SE) in brackets; cumulative percentage of the relative abundance of a growth form at a given depth (%); 95th percentile of the geometric size (Q95; cm^2); logarithmic mean size (Mean$_{log}$), and standard error (SE) in brackets; skewness (g_1) and statistic (Stat); kurtosis (g_2) and statistic (Stat); coefficient of variation (CV); probability of being normally distributed (p). Significance for g_1 and g_2: $|Stat| > 1.96$. Significant p-value < 0.05 (in bold).

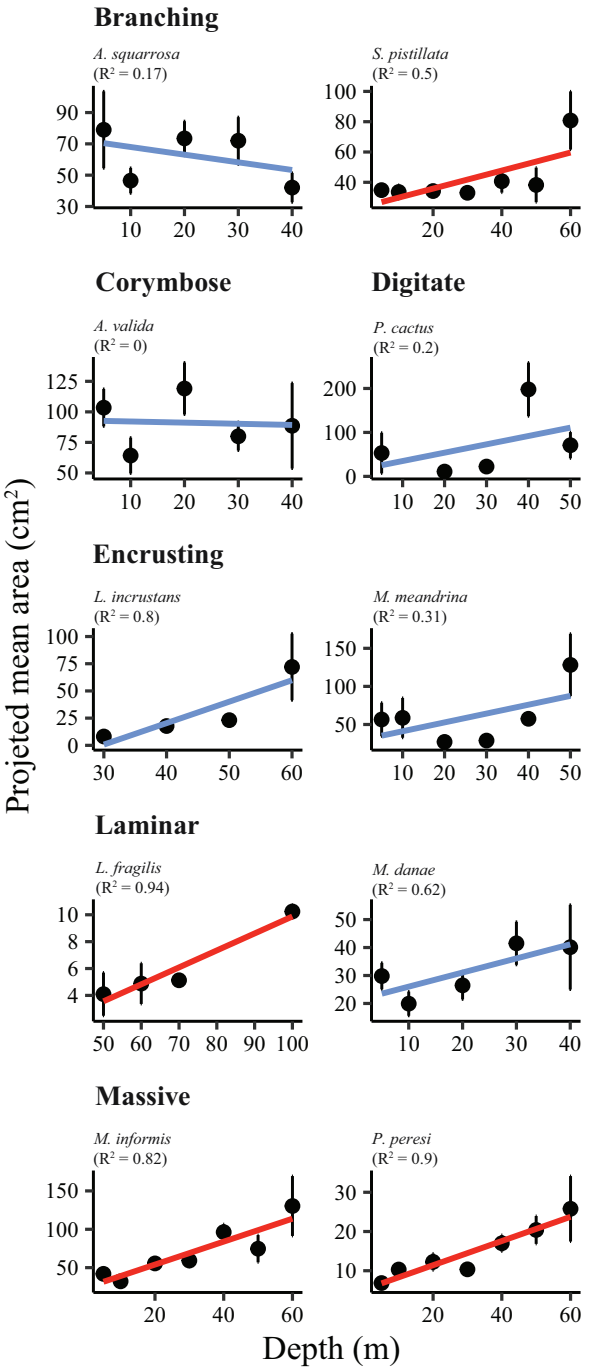

FIGURE 5 | Mean projected area (mean$_g$; cm^2) of ten representative locally abundant scleractinian corals belonging to six morphological categories, along a depth gradient. Red trendlines denote significant correlation ($p < 0.05$). The coefficient of determination (R^2) is given in brackets.

SFDs of Representative Species

The ten representative coral species exhibited heterogeneity in their size-structure with marked differences among depths and species (AD test, $p < 0.001$; **Figure 4**). Generally, mesophotic individuals tended to exhibit larger colony sizes (i.e., greater mean$_g$), but only four species showed a significant trend (**Figure 5** and **Table 2**). Nevertheless, some mesophotic species were typified by higher numbers of small colonies. Likewise, the coral species exhibited an increase in the 95th percentile and mean$_g$ with depth, especially at mesophotic depths (**Supplementary Figure S2**). *S. pistillata* exhibited no variation in mean$_g$ between 5 and 50 m (mean$_g$ = 33–41 cm^2; **Table 2**), but at 60 m it increased significantly to 81 cm^2 (permutational *t*-test, $p < 0.05$). Acroporidae corals did not display any clear trends of size across depth (**Figure 5**).

Excluding the Acroporidae corals, all other species exhibited different size-distributions between certain depths within a species (AD test, $p < 0.05$; **Table 2**). For several species, such as *A. squarrosa*, *P. peresi*, and *P. cactus*, the shallow SFDs were homogeneous, whereas *S. pistillata* SFDs were mostly homogeneous at mid-reef to upper mesophotic depths (20–60 m). On the whole, the distribution shapes were potentially symmetrical, especially for the massive and encrusting corals. Depth-generalists with a wide depth distribution (e.g., *S. pistillata* and *P. peresi*) were represented by colonies with smaller-size classes mostly in shallow waters, and generally exhibited lower dispersions of the size data (**Table 2**). However, depth-specialists such as the mesophotic *L. fragilis*, displayed dissimilar populations among depths, as indicated also by the high coefficient of variation (CV > 100). The overall CV significantly differed among the species (MEPA, $p < 0.001$), with the lowest values for *Acropora* spp. and *S. pistillata*, and the highest for *L. fragilis* and *P. peresi*.

Distributions displayed variable kurtosis degrees, and were negative for the shallow *S. pistillata* corals, reflecting that the outlier character (as measured by large |Z| -values) of the distribution is less extreme than that of a normal distribution. By contrast, deep massive-shaped and laminar coral species showed higher kurtosis values. Additionally, kurtosis varied among species within their depth-distributed populations but did not show any significant differences in species-specific corals with depth (permutational *t*-tests, $p > 0.05$; **Table 2**).

DISCUSSION

The present study compared the size-frequency distributions at the morphology level (six growth forms) and for locally abundant representatives coral species, along a wide depth gradient, from the shallow reef to the mesophotic ecosystem. As shown in previous studies, the size-structure of scleractinian coral populations is often linked to various environmental conditions, such as temperature, hydrodynamic regimes, and light (Vermeij and Bak, 2003; Bauman et al., 2013; Adjeroud et al., 2015; Goodbody-Gringley et al., 2015). Overall, the reefs along the shore of Eilat are characterized by heterogonous SFDs, dominated mostly by a higher number of small colonies. Nonetheless, the SFDs exhibited a wide distribution pattern among and within morphological categories and species, as well as along the depth gradient. Variations in a species' size-structure among depths within the same reef were previously

TABLE 2 | Basic statistical summary of untransformed data (white background) and statistical summary of SFD log-transformed colony size (shaded background) based on ten representative species (ordered by growth forms).

Growth form	Depth (m)	*n*	Mean$_g$ (SE)	%	Q95	Mean$_{log}$ (SE)	g_1 (Stat)	g_2 (Stat)	CV	*p*
A. squarrosa	5	18	79.00 (24.53)	3.3	297.66	1.49 (0.15)	0.09 (0.17)	−1.15 (−1.11)	67.06	1.00
	10	18	46.52 (8.09)	4.3	104.33	1.55 (0.08)	0.11 (0.21)	−1.24 (−1.20)	64.37	1.00
	20	59	73.48 (11.02)	7.8	283.71	1.58 (0.07)	−0.35 (−1.13)	−0.31 (−0.51)	63.24	1.00
	30	52	72.00 (15.05)	5.1	282.93	1.47 (0.08)	0.26 (0.78)	−0.52 (−0.79)	67.96	0.43
	40	29	42.08 (9.37)	4.3	165.43	1.34 (0.10)	0.1 (0.21)	−0.78 (−0.93)	74.76	1.00
S. pistillata	5	327	34.83 (3.64)	6.8	146.66	1.18 (0.10)	0.33 (2.99)	−0.40 (−2.55)	88.91	**0.01**
	10	179	33.60 (4.69)	24.6	133.91	1.53 (0.12)	0.40 (−0.71)	−0.68 (−2.06)	93.54	**0.00**
	20	185	34.22 (3.65)	24.5	118.20	1.19 (0.04)	−0.13 (0.17)	−0.75 (−2.30)	83.69	**0.01**
	30	245	33.07 (2.98)	11.1	123.61	1.15 (0.07)	0.03 (2.33)	−0.82 (−2.87)	85.94	**0.04**
	40	75	40.71 (7.51)	59.8	176.27	1.12 (0.03)	0.36 (2.15)	−0.89 (−0.72)	86.95	0.09
	50	33	38.26 (11.42)	43.4	149.81	1.07 (0.05)	0.60 (0.39)	−0.39 (−1.69)	84.43	0.99
	60	28	80.79 (19.22)	24.2	231.39	1.16 (0.04)	0.16 (0.21)	−1.35 (−1.34)	65.29	0.57
A. valida	5	74	103.45 (15.27)	13.5	375.02	1.66 (0.07)	−0.16 (−0.58)	−0.68 (−1.24)	60.11	1.00
	10	52	64.25 (14.63)	12.6	334.79	1.35 (0.09)	0.03 (0.09)	−0.34 (−0.52)	74.12	1.00
	20	73	119.11 (21.25)	9.7	571.32	1.67 (0.07)	0.16 (0.57)	−0.80 (−1.45)	59.87	1.00
	30	77	80.01 (11.61)	7.6	296.25	1.58 (0.07)	−0.25 (−0.93)	−0.48 (−0.88)	63.19	1.00
	40	13	88.61 (34.96)	1.9	308.33	1.56 (0.17)	0.55 (0.90)	−1.28 (−1.07)	64.24	0.45
P. cactus	5	4	53.04 (46.28)	0.7	164.70	1.15 (0.40)	1.46 (0.75)	2.40 (0.09)	87.10	1.00
	20	82	22.37 (9.2)	10.1	46.25	1.52 (0.10)	0.76 (1.69)	0.23 (1.64)	119.42	1.00
	30	68	197.83 (61.08)	2.9	988.30	1.26 (0.21)	0.86 (2.20)	1.63 (−0.86)	110.96	**0.02**
	40	14	70.88 (29.87)	8.1	296.12	0.90 (0.06)	0.58 (0.72)	−0.45 (−1.74)	65.94	**0.04**
	50	41	8.12 (1.40)	4.1	22.80	0.72 (0.06)	0.21 (0.56)	−1.00 (−0.35)	79.24	1.00
L. incrustans	30	130	17.75 (2.25)	19.2	52.78	0.98 (0.04)	0.39 (0.49)	−0.51 (−0.38)	138.16	1.00
	40	323	23.16 (2.20)	13.2	92.57	1.55 (0.13)	0.18 (1.73)	−0.28 (−1.25)	101.59	1.00
	50	15	72.04 (30.55)	3.3	264.97	1.43 (0.12)	0.37 (5.56)	−0.53 (2.25)	100.75	**0.00**
	60	18	56.57 (22.06)	3.1	195.44	1.47 (0.15)	0.75 (−1.18)	0.61 (0.58)	64.57	1.00
M. meandrina	5	13	58.72 (26.09)	15.2	184.80	1.19 (0.04)	0.47 (−0.95)	0.23 (1.92)	69.76	1.00
	10	115	27.13 (3.50)	15.1	71.44	1.27 (0.03)	−0.51 (0.32)	1.99 (−0.17)	67.84	0.56
	20	153	28.88 (2.65)	22.2	87.78	1.54 (0.04)	0.20 (0.25)	−0.20 (0.53)	84.06	1.00
	30	150	57.49 (5.32)	6.4	189.99	1.69 (0.12)	0.06 (−0.18)	0.24 (−1.13)	78.87	1.00
	40	31	128.20 (40.93)	66.7	436.26	0.99 (0.03)	−0.03 (−1.88)	−0.44 (1.95)	65.07	1.00
	50	13	4.09 (1.61)	2.9	12.51	1.38 (0.08)	−0.37 (0.12)	0.77 (0.74)	59.01	1.00
L. fragilis	50	52	4.88 (1.51)	9.4	11.07	1.00 (0.08)	1.74 (2.83)	3.34 (2.81)	235.36	**0.05**
	60	504	5.13 (0.24)	8.9	14.00	1.06 (0.07)	1.61 (4.88)	4.16 (6.41)	227.36	**0.00**
	70	407	10.24 (0.49)	8.7	30.21	1.23 (0.06)	0.44 (4.03)	−0.19 (−0.86)	178.51	**0.00**
	100	16	29.80 (4.73)	2.5	60.97	1.24 (0.14)	−0.09 (−0.76)	−0.77 (−3.17)	120.65	**0.00**
M. danae	5	39	19.92 (4.32)	2.7	76.37	0.42 (0.10)	−0.68 (0.06)	0.65	72.25	1.00
	10	67	26.47 (5.01)	45.6	108.89	0.44 (0.05)	0.03 (1.08)	−0.49	99.89	1.00
	20	88	41.50 (7.68)	100	196.10	0.83 (0.02)	0.41 (1.23)	−0.41	93.96	0.56
	30	17	40.12 (15.13)	100	163.21	0.56 (0.02)	0.36 (0.58)	−0.27	80.99	0.84
	40	55	41.92 (8.34)	10.1	133.69	1.34 (0.07)	0.15 (0.21)	−0.08	80.96	1.00
M. informis	5	29	32.18 (7.29)	7	104.94	1.20 (0.10)	0.12 (−0.20)	−0.13	74.67	1.00
	10	95	55.51 (7.84)	12.6	232.95	1.41 (0.06)	−0.06 (0.70)	−0.64	83.32	1.00
	20	145	59.25 (8.12)	12.7	174.73	1.76 (0.05)	0.30 (0.28)	−0.81	71.05	0.08
	30	86	96.29 (10.40)	6.4	318.71	1.46 (0.01)	0.07 (−2.03)	−0.07	67.03	1.00
	40	31	74.69 (17.79)	5.3	294.73	1.99 (0.16)	−0.41 (0.19)	−0.16	56.67	1.00
	50	6	130.34 (39.01)	6.4	252.13	0.72 (0.05)	0.05 (−0.76)	−0.88	68.44	1.00
	60	35	6.86 (0.99)	12.7	17.32	0.79 (0.04)	−0.32 (0.56)	−1.50	50.20	1.00
P. peresi	5	82	10.31 (1.31)	16	27.11	0.96 (0.05)	0.05 (0.51)	0.60	137.98	1.00
	10	138	12.26 (2.15)	8.1	41.01	1.07 (0.08)	0.20 (2.91)	−0.60	124.03	1.00
	20	129	10.36 (1.22)	11.4	34.19	1.14 (0.14)	0.77 (2.28)	0.71	127.29	**0.00**
	30	108	17.00 (2.10)	19.8	58.91	0.81 (0.05)	0.47 (1.50)	−0.38	127.12	0.06
	40	39	20.40 (3.55)	18.3	65.02	0.79 (0.04)	0.32 (0.26)	−0.57	104.49	0.30
	50	13	25.78 (8.35)	14.3	84.52	1.49 (0.04)	0.06 (0.49)	−0.81	93.21	1.00
	60	18	79.00 (24.53)	3.3	297.66	1.49 (0.15)	0.18 (2.37)	−0.11	87.52	1.00

The sample size (n); geometric mean size (Mean$_g$; cm^2) and standard error (SE) in brackets; cumulative percentage of the relative abundance of a growth form at a given depth (%); 95th percentile of the geometric size (Q95; cm^2); logarithmic mean size (Mean$_{log}$) and standard error (SE) in brackets; skewness (g_1) and statistic (Stat); kurtosis (g_2) and statistic (Stat); coefficient of variation (CV); probability of being normally distributed (p). Significance for g_1 and g_2: $|Stat| > 1.96$. Significant p-value < 0.05 (in bold).

demonstrated at sites from French Polynesia (Adjeroud et al., 2007, 2015) and the Maldives (Lasagna et al., 2010). However, those studies were limited to the shallow part of the reef at a maximal depth of 18 meters. "Generalist" zooxanthellate stony coral species may be distributed from shallows down to the mesophotic depths (100 m in clear waters), whereas "depth-specialist" species can be found exclusively in either the shallow or the deep parts of the reef (Lesser et al., 2010; Laverick et al., 2017; Tamir et al., 2019). Hence, assessing species size-structure patterns along the shallow-mesophotic depth gradient is necessary in order to obtain improved knowledge on coral population distribution patterns and their life-history processes, which will, in turn, lead to a more accurate indication of their health and stability. In essence, characterizing a given species only at a certain depth may be misleading when seeking to assess crucial life-history factors, such as recruitment, fecundity, mortality, and population turnover (Shlesinger et al., 2018; Kramer et al., 2019).

Mean colony size may indicate the response of a species to the environment (Fisher et al., 2008). Here we measured colony size as projected surface area, which can serve as an effective proxy for three-dimensional colony size (House et al., 2018). Two growth forms, corymbose and encrusting, appeared to be insensitive to depth (**Table 1**), i.e., did not show significant variations in $mean_g$ along the depth gradient. Of all the studied growth forms, the corymbose corals revealed the most constrained coral size at all depths, with lower variance in size. This group, which mainly consists of *Acropora* species, is known as a highly sensitive group to environmental anomalies (Madin et al., 2014; Hughes et al., 2017). In a recent study, a member of the corymbose group (*Acropora eurostoma;* 0–10 m), along with species from other growth forms, exhibited a breakdown in reproductive synchronization in the GoE/A (Shlesinger and Loya, 2019). As evident also from our present findings (**Table 1**; *A. valida* in **Table 2**), the lack of smaller-size groups raises concerns regarding the future of corymbose populations not only at shallow depths of the GoE/A but also at mesophotic depths, and may imply that they are at risk of decline due to the lack of new recruits (Bak and Meesters, 1998).

Regardless of the general decline in coral size with depth, we nonetheless detected marked differences among most of the studied representative species populations across depths. In comparison to the shallow-water colonies, mesophotic corals were associated with larger $mean_g$ and the 95th percentile. The larger colony sizes of corals inhabiting the mesophotic depths may indicate longer survival, and longer period of growth. This is probably possible due to their experiencing fewer of the disturbances that prevent corals from reaching their maximal potential size (Lesser et al., 2009). Such phenomena suggest that the mesophotic reefs of Eilat may have a potential role as a stable and sheltered environment for scleractinian corals, since corals can reach greater sizes there. However, these conclusions should be approached with caution, since there is evidence that the mesophotic reefs too may not always escape climate-induced disturbances (Eyal et al., 2019; Pinheiro et al., 2019). Indeed, since the mesophotic reefs comprise mostly slow-growing coral growth forms (e.g., encrusting), they are expected to require longer recovery periods after major disturbances, although they are generally considered more robust to physical and thermal stress (Torda et al., 2018).

Although on average larger colonies were observed in the MCEs, in most cases the coral species at these depths exhibited balanced population size-structures. It is widely accepted that mesophotic coral species have slower growth rates than their shallow congeners, since light, the primary energy source, is decreasing exponentially with depth (Kirk, 2011; Lesser et al., 2018; Kahng et al., 2019). Slower growth rates at the mesophotic depths are further linked to the dominant growth forms prevalent at these depths (Kahng et al., 2019). Plate-like and encrusting coral growth forms have been long known to exhibit slower growth rates and are typically more abundant at deeper habitats (Buddemeier and Kinzie, 1976; Fricke and Meischner, 1985). For shallow reefs, the coral contribution is largely due to fast-growing corals, such as branching and corymbose, which are common coral morphologies in many shallow-water reefs; whereas at the mesophotic depths the coral contribution may result from a combination of high environmental stability and slow-growing morphologies, which are considered to be more tolerant to stressful environments (Darling et al., 2012), consequently allowing coral populations to achieve balanced and stable size-populations. Moreover, corals in low-light environments (e.g., mesophotic) maximize their surface area at the colony morphological level, thus maximizing their light reception (Hughes and Jackson, 1985; Lesser et al., 2010; Einbinder et al., 2016). Consequently, encrusting, laminar, and massive morphologies are better fitted to survive and flourish under such extreme optical conditions, although some branching and digitate depth-generalist species are known to adjust their morphology (i.e., becoming flatter) with depth (Eyal et al., 2015, 2019; Einbinder et al., 2016; Kahng et al., 2019). This corresponds to the DistLM test, which found light (PAR) to be a significant environmental factor affecting the size-distribution of corals. Nevertheless, we found that light explains only 10% of the variation, suggesting that biotic factors might have a greater contribution. For example, a lack of suitable competitors that can also withstand the unique mesophotic conditions, particularly during their early-life stages (Álvarez-Noriega et al., 2018), allows corals to grow without suppression from such neighboring competitors. Additionally, demographic traits (such as growth rate) that are linked to a species' life-history strategies may affect its size-distribution.

Life-history strategies correspond to marked differences among different morphological size distributions (Darling et al., 2012). The branching colonies studied here exhibited positively skewed populations and platykurtic distributions only at shallow depths, while at mesophotic depths they were symmetrical. Unfortunately, previous coral-reef surveys of Eilat's reefs did not include population structure data along the mesophotic depth slope; and therefore, we could not compare this study to any earlier documentation. Nonetheless, the findings from

our study match previous reports from other geographical regions. A study from Curaçao, for example, on the population structure of different morphologies of the *Madracis* genus along a depth gradient, showed a higher dominancy of smaller-size classes in branched species at shallow depths (Vermeij and Bak, 2003). Shallow reefs are considered less predictable environments due to higher frequencies of disturbances, which may result in higher occurrences of smaller-size groups, particularly for typically "weedy" species such as branching corals with a high population turnover (Loya, 1976, 2004; Darling et al., 2012). Whether the lack of smaller-size groups at the mesophotic depths, such as seen in *S. pistillata* in this study, is a result of lower reproductive performance (Shlesinger et al., 2018) or low survival at these depths (Kramer et al., 2019), requires further investigation. Similar to our findings for massive corals, a study of Bermuda's reefs revealed that the massive mesophotic *Montastraea cavernosa* populations were positively skewed toward smaller individuals (Goodbody-Gringley et al., 2015). As noted above, encrusting, laminar, and massive growth forms commonly exhibit slower growth rates than other growth forms, and therefore a slower transition through the size-classes (Pratchett et al., 2015). In comparison, branched colonies display a low kurtosis, reflecting a faster transition to larger-size classes.

An unexpected discovery resulting from the analysis of the coral species abundance across the 5–100 m depth was that of the surprising dominancy of *L. glabra* in the GoE/A. For decades, it was widely accepted that *S. pistillata* was the most abundant species in our study area; i.e., surveys beginnings in the early 1970s and on (Loya, 1972, 1976, 2004; NMP, 2017), have shown this species to be the most widely distributed and most abundant coral in the northern GoE/A. Thus, the numerous studies that were performed in shallow reef zones (i.e., not exceeding 30 m depth) have rightfully accepted this assertion. However, in the current study when the data is examined among all sites and takes into account the whole depth gradient (down to 100 m), *L. glabra* is, in fact, nearly two-fold more abundant than *S. pistillata*. Nonetheless, the occurrence of *Leptoseris* species, and particularly *L. glabra*, is restricted to mesophotic depths. *Leptoseris* species are key members of the mesophotic reefs, not only in the Red Sea (Tamir et al., 2019), but also in other regions worldwide, e.g., Hawaii (Spalding et al., 2019) and Australia (Englebert et al., 2017). A combination of the unique environmental adaptations (Fricke et al., 1987; Kahng et al., 2012), the lack of suitable competitors, and a larger potential habitat availability for settlement (MCEs comprise ˜80% of coral reef habitats (Pyle and Copus, 2019; Kramer et al., 2019), may allow *Leptoseris* spp. to thrive in mesophotic depths and significantly contribute to its high abundance and coral living coverage.

Overall, our findings indicate that although the shallow and mesophotic reefs of Eilat support established and balanced structured populations of multiple depth-generalists, nonetheless, as recently suggested, there are concerns regarding the future of corymbose corals (Shlesinger and Loya, 2019). Furthermore, changes in light conditions (i.e., depth) exert different effects on the size-structures and spatial distribution of growth forms and species' populations. Future studies should focus on important life-history traits, such as skeletal growth rates and reproduction, particularly at the mesophotic depths, which will provide a more comprehensive understanding of the populations dwelling at these depths. In the coming decades, coral reefs are expected to confront multiple threats of increasing intensities and frequencies, and which are expected to dramatically shift the community compositions and population structures. Hence, the data provided by this study can serve as a baseline for future monitoring of coral population structures, providing important insights to recent ecological dynamics, as well as a retrospective assessment of coral community recovery following major disturbance events (Gilmour et al., 2013; Torda et al., 2018), and considerable ecological grounds for conservation assessments and management actions.

DATA AVAILABILITY STATEMENT

The raw data supporting the conclusions of this article will be made available by the authors, without undue reservation, to any qualified researcher.

AUTHOR CONTRIBUTIONS

NK, RT, GE, and YL conceived and designed the research. RT and GE conducted the fieldwork. NK and RT analyzed the field data and performed the statistical analysis. NK wrote the manuscript. All authors contributed to content revisions and approval of the final text.

FUNDING

This work was supported by the Israel Science Foundation (ISF) Grant No. 1191/16 to YL and by the European Union's Horizon 2020 under the Marie Skłodowska-Curie postdoctoral grant agreement no. 796025 to GE.

ACKNOWLEDGMENTS

We are grateful to the Interuniversity Institute for Marine Sciences in Eilat (IUI) for the logistical assistance, and to all the students at YL's lab for help in the fieldwork. We thank N. Paz for editing the manuscript.

SUPPLEMENTARY MATERIAL

The Supplementary Material for this article can be found online at: https://www.frontiersin.org/articles/10.3389/fmars.2020.00615/full#supplementary-material

REFERENCES

Adjeroud, M., Mauguit, Q., and Penin, L. (2015). The size-structure of corals with contrasting life-histories: a multi-scale analysis across environmental conditions. *Mar. Environ. Res.* 112, 131–139. doi: 10.1016/j.marenvres.2015.10.004

Adjeroud, M., Pratchett, M. S., Kospartov, M. C., Lejeusne, C., and Penin, L. (2007). Small-scale variability in the size structure of scleractinian corals around Moorea, French Polynesia: patterns across depths and locations. *Hydrobiologia* 598, 117–126. doi: 10.1007/s10750-007-0726-2

Álvarez-Noriega, M., Baird, A. H., Dornelas, M., Madin, J. S., and Connolly, S. R. (2018). Negligible effect of competition on coral colony growth. *Ecology* 99, 1347–1356. doi: 10.1002/ecy.2222

Anderson, K. D., and Pratchett, M. S. (2014). Variation in size-frequency distributions of branching corals between a tropical versus sub-tropical reef. *Mar. Ecol. Prog. Ser.* 502, 117–128. doi: 10.3354/meps10697

Baird, A. H., and Marshall, P. A. (2002). Mortality, growth and reproduction in scleractinian corals following bleaching on the Great Barrier Reef. *Mar. Ecol. Prog. Ser.* 237, 133–141. doi: 10.3354/meps237133

Bak, R. P. M., and Meesters, E. H. (1998). Coral population structure: the hidden information of colony size-frequency distributions. *Mar. Ecol. Prog. Ser.* 162, 301–306. doi: 10.3354/meps162301

Bak, R. P. M., and Meesters, E. H. (1999). Population structure as a response of coral communities to global change. *Am. Zool.* 39, 56–65. doi: 10.1093/icb/39.1.56

Bates, D., Mächler, M., Bolker, B., and Walker, S. (2015). Fitting linear mixed-effects models using {lme4}. *J. Stat. Softw.* 67, 1–48. doi: 10.18637/jss.v067.i01

Bauman, A. G., Pratchett, M. S., Baird, A. H., Riegl, B., Heron, S. F., and Feary, D. A. (2013). Variation in the size structure of corals is related to environmental extremes in the Persian Gulf. *Mar. Environ. Res.* 84, 43–50. doi: 10.1016/j.marenvres.2012.11.007

Bongaerts, P., Ridgway, T., Sampayo, E. M., and Hoegh-Guldberg, O. (2010). Assessing the "deep reef refugia" hypothesis: focus on Caribbean reefs. *Coral Reefs* 29, 1–19. doi: 10.1007/s00338-009-0581-x

Buddemeier, R. W., and Kinzie, R. A. (1976). Coral growth. *Oceanogr. Mar. Biol. Annu. Rev.* 14, 183–225.

Clarke, K. R. (1993). Non-parametric multivariate analyses of changes in community structure. *Aust. J. Ecol.* 18, 117–143. doi: 10.1111/j.1442-9993.1993.tb00438.x

Cramer, D. (1997). *Basic Statistics for Social Research: Step-by-step Calculations and Computer Techniques Using Minitab*. London: Routledge.

Darling, E. S., Alvarez-Filip, L., Oliver, T. A., McClanahan, T. R., and Côté, I. M. (2012). Evaluating life-history strategies of reef corals from species traits. *Ecol. Lett.* 15, 1378–1386. doi: 10.1111/j.1461-0248.2012.01861.x

Darling, E. S., McClanahan, T. R., and Côté, I. M. (2013). Life histories predict coral community disassembly under multiple stressors. *Glob. Chang. Biol.* 19, 1930–1940. doi: 10.1111/gcb.12191

Dubé, C. E., Mercière, A., Vermeij, M. J. A., and Planes, S. (2017). Population structure of the hydrocoral *Millepora platyphylla* in habitats experiencing different flow regimes in Moorea, French polynesia. *PLoS One* 12:e0173513. doi: 10.1371/journal.pone.0173513

Einbinder, S., Gruber, D. F., Salomon, E., Liran, O., Keren, N., and Tchernov, D. (2016). Novel adaptive photosynthetic characteristics of mesophotic symbiotic microalgae within the reef-building coral, *Stylophora pistillata*. *Front. Mar. Sci.* 3:195. doi: 10.3389/fmars.2016.00195

Einbinder, S., Mass, T., Brokovich, E., Dubinsky, Z., Erez, J., and Tchernov, D. (2009). Changes in morphology and diet of the coral Stylophora pistillata along a depth gradient. *Mar. Ecol. Prog. Ser.* 381, 167–174. doi: 10.3354/meps07908

Englebert, N., Bongaerts, P., Muir, P. R., Hay, K. B., Pichon, M., and Hoegh-Guldberg, O. (2017). Lower mesophotic coral communities (60-125 m depth) of the northern great barrier reef and coral sea. *PLoS One* 12:0170336. doi: 10.1371/journal.pone.0170336

Eyal, G., Eyal-Shaham, L., and Loya, Y. (2011). "Teeth-anchorage": sleeping behavior of a Red Sea filefish on a branching coral. *Coral Reefs* 30:707. doi: 10.1007/s00338-011-0766-y

Eyal, G., Tamir, R., Kramer, N., Eyal-shaham, L., and Loya, Y. (2019). "The Red Sea: israel," in *Mesophotic Coral Ecosystems*, eds Y. Loya, K. A. Puglise, and T. C. L. Bridge, (New York: Springer), 199–214.

Eyal, G., Wiedenmann, J., Grinblat, M., D'Angelo, C., Kramarsky-Winter, E., Treibitz, T., et al. (2015). Spectral diversity and regulation of coral fluorescence in a mesophotic reef habitat in the Red Sea. *PLoS One* 10:e0128697. doi: 10.1371/journal.pone.0128697

Fisher, W. S., Fore, L. S., Hutchins, A., Quarles, R. L., Campbell, J. G., LoBue, C., et al. (2008). Evaluation of stony coral indicators for coral reef management. *Mar. Pollut. Bull.* 56, 1737–1745. doi: 10.1016/j.marpolbul.2008.07.002

Fricke, H., and Meischner, D. (1985). Depth limits of *Bermudan scleractinian* corals: a submersible survey. *Mar. Biol.* 88, 175–187. doi: 10.1007/BF00397165

Fricke, H. W., and Schuhmacher, H. (1983). The depth limits of red sea stony corals: an ecophysiological problem (A deep diving survey by submersible). *Mar. Ecol.* 4, 163–194. doi: 10.1111/j.1439-0485.1983.tb00294.x

Fricke, H. W., Vareschi, E., and Schlichter, D. (1987). Photoecology of the coral *Leptoseris fragilis* in the Red Sea twilight zone (an experimental study by submersible). *Oecologia* 73, 371–381. doi: 10.1007/BF00385253

Gilmour, J. P., Smith, L. D., Heyward, A. J., Baird, A. H., and Pratchett, M. S. (2013). Recovery of an isolated coral reef system following severe disturbance. *Science* 340, 69–71. doi: 10.1126/science.1232310

Glynn, P. W. (1996). Coral reef bleaching: facts, hypotheses and implications. *Glob. Chang. Biol.* 2, 495–509. doi: 10.1111/j.1365-2486.1996.tb00063.x

Goodbody-Gringley, G., Marchini, C., Chequer, A. D., and Goffredo, S. (2015). Population structure of *Montastraea cavernosa* on shallow versus mesophotic reefs in Bermuda. *PLoS One* 10:e0142427. doi: 10.1371/journal.pone.0142427

Goreau, T. (1959). The physiology of skeleton formation in corals. I. A method for measuring the rate of calcium deposition by corals under different conditions. *Biol. Bull.* 116, 59–75. doi: 10.2307/1539156

Hervé, M. (2019). *RVAideMemoire: Testing and Plotting Procedures for Biostatistics. R package version 0.9–73*.

Hinderstein, L. M., Marr, J. C. A., Martinez, F. A., Dowgiallo, M. J., Puglise, K. A., Pyle, R. L., et al. (2010). Theme section on "Mesophotic coral ecosystems: characterization, ecology, and management.". *Coral Reefs* 29, 247–251. doi: 10.1007/s00338-010-0614-5

House, J. E., Brambilla, V., Bidaut, L. M., Christie, A. P., Pizarro, O., Madin, J. S., et al. (2018). Moving to 3D: relationships between coral planar area, surface area and volume. *PeerJ* 6:e4280. doi: 10.7717/peerj.4280

Hughes, T. P., Anderson, K. D., Connolly, S. R., Heron, S. F., Kerry, J. T., Lough, J. M., et al. (2018a). Spatial and temporal patterns of mass bleaching of corals in the Anthropocene. *Science* 359, 80–83. doi: 10.1126/science.aan8048

Hughes, T. P., and Jackson, J. B. C. (1985). Population dynamics and life histories of foliaceous corals. *Ecol. Monogr.* 55, 141–166. doi: 10.2307/1942555

Hughes, T. P., Kerry, J. T., Álvarez-Noriega, M., Álvarez-Romero, J. G., Anderson, K. D., Baird, A. H., et al. (2017). Global warming and recurrent mass bleaching of corals. *Nature* 543, 373–377.

Hughes, T. P., Kerry, J. T., Baird, A. H., Connolly, S. R., Dietzel, A., Eakin, C. M., et al. (2018b). Global warming transforms coral reef assemblages. *Nature* 556, 492–496. doi: 10.1038/s41586-018-0041-2

Kahng, S. E., Akkaynak, D., Shlesinger, T., Hochberg, E. J., Wiedenmann, J., Tamir, R., et al. (2019). "Light, temperature, photosynthesis, heterotrophy, and the lower depth limits of mesophotic coral ecosystems," in *Mesophotic Coral Ecosystems*, eds Y. Loya, K. A. Puglise, and T. C. L. Bridge, (Cham: Springer International Publishing), 801–828. doi: 10.1007/978-3-319-92735-0_42

Kahng, S. E., Hochberg, E. J., Apprill, A., Wagner, D., Luck, D. G., Perez, D., et al. (2012). Efficient light harvesting in deep-water zooxanthellate corals. *Mar. Ecol. Prog. Ser.* 455, 65–77. doi: 10.3354/meps09657

Katz, T., Ginat, H., Eyal, G., Steiner, Z., Braun, Y., Shalev, S., et al. (2015). Desert flash floods form hyperpycnal flows in the coral-rich Gulf of Aqaba, Red Sea. *Earth Planet. Sci. Lett.* 417, 87–98. doi: 10.1016/j.epsl.2015.02.025

Kirk, J. T. O. (2011). *Light and Photosynthesis in Aquatic Ecosystems*, 3rd Edn. New York: Cambridge University Press.

Kramer, N., Eyal, G., Tamir, R., and Loya, Y. (2019). Upper mesophotic depths in the coral reefs of Eilat, Red Sea, offer suitable refuge grounds for coral settlement. *Sci. Rep.* 9:2263. doi: 10.1038/s41598-019-38795-1

Lasagna, R., Albertelli, G., Morri, C., and Bianchi, C. N. (2010). Acropora abundance and size in the Maldives six years after the 1998 mass mortality: patterns across reef typologies and depths. *J. Mar. Biol. Assoc. U. K.* 90, 919–922. doi: 10.1017/S0025315410000020

Laverick, J. H., Andradi-Brown, D. A., and Rogers, A. D. (2017). Using light-dependent scleractinia to define the upper boundary of mesophotic coral

ecosystems on the reefs of Utila, Honduras. *PLoS One* 12:e0183075. doi: 10.1371/journal.pone.0183075

Lazar, B., Erez, J., Silverman, J., Rivlin, T., Rivlin, A., Dray, M., et al. (2008). Recent environmental changes in the chemical-biological oceanography of the Gulf of Aqaba (Eilat). Aqaba-Eilat, Improbable Gulf. *Environ. Biodivers. Preserv. Environ.* 49–61.

Lesser, M. P., Marc, S., Michael, S., Michiko, O., Gates, R. D., and Andrea, G. (2010). Photoacclimatization by the coral *Montastraea cavernosa* in the mesophotic zone: light, food, and genetics. *Ecology* 91, 990–1003. doi: 10.1890/09-0313.1

Lesser, M. P., Slattery, M., and Leichter, J. J. (2009). Ecology of mesophotic coral reefs. *J. Exp. Mar. Bio. Ecol.* 375, 1–8. doi: 10.1016/j.jembe.2009.05.009

Lesser, M. P., Slattery, M., and Mobley, C. D. (2018). Biodiversity and functional ecology of mesophotic coral reefs. *Annu. Rev. Ecol. Evol. Syst.* 49, 49–71. doi: 10.1146/annurev-ecolsys-110617-062423

Loya, Y. (1972). Community Structure and species diversity of hermatypic corals at Eilat, Red Sea. *Mar. Biol.* 13, 100–123. doi: 10.1007/bf00366561

Loya, Y. (1976). The Red Sea coral Stylophora pistillata is an r strategist. *Nature* 259, 478–480. doi: 10.1038/260170a0

Loya, Y. (2004). "The coral reefs of eilat — past, present and future: three decades of coral community structure studies," in *Coral Health and Disease*, eds E. Rosenberg, and Y. Loya, (Berlin: Springer), 1–34. doi: 10.1007/978-3-662-06414-6_1

Loya, Y. (2007). How to influence environmental decision makers? The case of Eilat (Red Sea) coral reefs. *J. Exp. Mar. Bio. Ecol.* 344, 35–53. doi: 10.1016/j.jembe.2006.12.005

Loya, Y., Eyal, G., Treibitz, T., Lesser, M. P., and Appeldoorn, R. (2016). Theme section on mesophotic coral ecosystems: advances in knowledge and future perspectives. *Coral Reefs* 35, 1–9. doi: 10.1007/s00338-016-1410-7

Loya, Y., Puglise, K. A., and Bridge, T. C. L. (eds) (2019). *Mesophotic Coral Ecosystems*. New York: Springer.

Loya, Y., Sakai, K., Yamazato, K., Nakano, Y., Sambali, H., and Van Woesik, R. (2001). Coral bleaching: the winners and the losers. *Ecol. Lett.* 4, 122–131. doi: 10.1046/j.1461-0248.2001.00203.x

Luo, D., Ganesh, S., and Koolaard, J. (2014). *predictmeans: Calculate Predicted Means for Linear Models 1.0.4*.

Madin, J. S., Anderson, K. D., Andreasen, M. H., Bridge, T. C. L., Cairns, S. D., Connolly, S. R., et al. (2016). The Coral Trait Database, a curated database of trait information for coral species from the global oceans. *Sci. Data* 3:160017. doi: 10.1038/sdata.2016.17

Madin, J. S., Baird, A. H., Dornelas, M., and Connolly, S. R. (2014). Mechanical vulnerability explains size-dependent mortality of reef corals. *Ecol. Lett.* 17, 1008–1015. doi: 10.1111/ele.12306

Neal, B. P., Khen, A., Treibitz, T., Beijbom, O., O'Connor, G., Coffroth, M. A., et al. (2017). Caribbean massive corals not recovering from repeated thermal stress events during 2005–2013. *Ecol. Evol.* 7, 1339–1353. doi: 10.1002/ece3.2706

NMP (2017). *Inter University Institute for Marine Sciences in Eilat*. Available online at: http://www.meteotech.co.il/EilatYam_data/ey_surface_coastal_cruise_download_data.asp

Oksanen, J., Blanchet, F. G., Friendly, M., Kindt, R., Legendre, P., McGlinn, D., et al. (2018). *vegan: Community Ecology Package. R package version 2.4–6*.

Osborne, K., Thompson, A. A., Cheal, A. J., Emslie, M. J., Johns, K. A., Jonker, M. J., et al. (2017). Delayed coral recovery in a warming ocean. *Glob. Chang. Biol.* 23, 3869–3881. doi: 10.1111/gcb.13707

Pinheiro, H. T., Eyal, G., Shepherd, B., and Rocha, L. A. (2019). Ecological insights from environmental disturbances in mesophotic coral ecosystems. *Ecosphere* 10:e02666. doi: 10.1002/ecs2.2666

Pratchett, M. S., Anderson, K. D., Hoogenboom, M. O., Widman, E., Baird, A. H., Pandolfi, J. M., et al. (2015). Spatial, temporal and taxonomic variation in coral growth–implications for the strucutre and function of coral reef ecosystems. *Oceanogr. Mar. Biol. An. Annu. Rev.* 53, 215–296.

Pyle, R. L., and Copus, J. M. (2019). "Mesophotic coral ecosystems: introduction and overview," in *Mesophotic Coral Ecosystems*, eds Y. Loya, K. A. Puglise, and T. C. L. Bridge, (New York: Springer).

R Core Team, (2020). *R: A Language and Environment for Statistical Computing*. Vienna: R Foundation for Statistical Computing.

Rocha, L. A., Pinheiro, H. T., Shepherd, B., Papastamatiou, Y. P., Luiz, O. J., Pyle, R. L., et al. (2018). Mesophotic coral ecosystems are threatened and ecologically distinct from shallow water reefs. *Science* 361, 281–284. doi: 10.1126/science.aaq1614

Shlesinger, T., Grinblat, M., Rapuano, H., Amit, T., and Loya, Y. (2018). Can mesophotic reefs replenish shallow reefs? Reduced coral reproductive performance casts a doubt. *Ecology* 99, 421–437. doi: 10.1002/ecy.2098

Shlesinger, T., and Loya, Y. (2019). Breakdown in spawning synchrony: a silent threat to coral persistence. *Science* 365, 1002–1007. doi: 10.1126/science.aax0110

Smith, L. D., Devlin, M., Haynes, D., and Gilmour, J. P. (2005). A demographic approach to monitoring the health of coral reefs. *Mar. Pollut. Bull.* 51, 399–407. doi: 10.1016/j.marpolbul.2004.11.021

Spalding, H. L., Copus, J. M., Bowen, B. W., Kosaki, R. K., Longenecker, K., Montgomery, A. D., et al. (2019). "The Hawaiian archipelago," in *Mesophotic Coral Ecosystems*, eds Y. Loya, K. A. Puglise, and T. C. L. Bridge, (Cham: Springer International Publishing), 445–464.

Tamir, R., Eyal, G., Kramer, N., Laverick, J. H., and Loya, Y. (2019). Light environment drives the shallow to mesophotic coral community transition. *Ecosphere* 10:e02839. doi: 10.1101/622191

Tamir, R., Lerner, A., Haspel, C., Dubinsky, Z., and Iluz, D. (2017). The spectral and spatial distribution of light pollution in the waters of the northern Gulf of Aqaba (Eilat). *Sci. Rep.* 7:42329. doi: 10.1038/srep42329

Torda, G., Sambrook, K., Cross, P., Sato, Y., Bourne, D. G., Lukoschek, V., et al. (2018). Decadal erosion of coral assemblages by multiple disturbances in the Palm Islands, central Great Barrier Reef. *Sci. Rep.* 8, 1–10. doi: 10.1038/s41598-018-29608-y

Turner, J. A., Babcock, R. C., Hovey, R., and Kendrick, G. A. (2017). Review Article Deep thinking?: a systematic review of mesophotic coral ecosystems. *ICES J. Mar. Sci.* 74, 2309–2320. doi: 10.1093/icesjms/fsx085

Vermeij, M. J. A., and Bak, R. P. M. (2003). Species-specific population structure of closely related coral morphospecies along a depth gradient (5-60 M) over a Caribbean reef slope. *Bull. Mar. Sci.* 73, 725–744.

Zakai, D., and Chadwick-furman, N. E. (2002). Impacts of intensive recreational diving on reef corals at Eilat. *Biol. Conserv.* 105, 179–187. doi: 10.1016/s0006-3207(01)00181-1

Zawada, K. J. A., Dornelas, M., and Madin, J. S. (2019). Quantifying coral morphology. *Coral Reefs* 38, 1281–1292. doi: 10.1007/s00338-019-01842-4

Zvuloni, A., Artzy-Randrup, Y., Stone, L., van Woesik, R., and Loya, Y. (2008). Ecological size-frequency distributions: how to prevent and correct biases in spatial sampling. *Limnol. Oceanogr. Methods* 6, 144–153. doi: 10.4319/lom.2008.6.144

Conflict of Interest: The authors declare that the research was conducted in the absence of any commercial or financial relationships that could be construed as a potential conflict of interest.